MIMO-UFMC Transceiver Schemes for Millimeter Wave Wireless Communications

Stefano Buzzi[1(✉)], Carmen D'Andrea[1], Dejian Li[2], and Shulan Feng[2]

[1] University of Cassino and Southern Lazio, Cassino, Italy
{buzzi,carmen.dandrea}@unicas.it
[2] Hisilicon Technologies Co., Ltd, Beijing, People's Republic of China
{lidejian,Shulan.Feng}@hisilicon.com

Abstract. This paper provides results on the use of UFMC modulation scheme in MIMO wireless links operating at mmWave frequencies. First of all, full mathematical details on the processing needed to realize a MIMO-UFMC transceiver at mmWave, taking into account also the hybrid analog/digital nature of the beamformers, are given. Then, we propose several reception structures, considering also the case of continuous packet transmission with no guard intervals among the packets. In particular, an adaptive low complexity MMSE receiver is proposed that is shown to achieve very satisfactory performance. A channel independent transmit beamformer is also considered, as as to avoid the need for channel state information at the transmitter. Numerical results show that the proposed transceiver schemes are effective, as well as that the continuous packet transmission scheme, despite increased interference, attains the highest values of system throughput.

Keywords: MIMO-UFMC · Millimeter waves · 5G Networks

1 Introduction

The Universal Filtered MultiCarrier (UFMC), one of the modulations that is considered as an alternative to orthogonal frequency division multiplexing (OFDM) for future wireless systems [2], is an intermediate scheme between filtered-OFDM and Filter Bank MultiCarrier (FBMC). Indeed, while in filtered OFDM the whole OFDM signal is filtered to reduce OOB emissions and achieve better spectral containment [1], and while in FBMC each subcarrier is individually filtered [5], in UFMC the subcarriers are grouped in contiguous, non-overlapping blocks, called *subbands*, and each subband is individually filtered [7].

This paper has been supported by Huawei through HIRP OPEN Agreement No. HO2016050002BM.

X. Liu et al. (Eds.): ChinaCom 2018, LNICST 262, pp. 14–23, 2019.
https://doi.org/10.1007/978-3-030-06161-6_2

UFMC has been received an increasing attention is the last few years; however, despite the relevance of multi-antenna processing to future fifth-generation (5G) wireless systems, its use in conjunction with a multiple-input-multiple-output (MIMO) configuration has not been fully addressed in the open literature; similarly, the potentialities coming from the use of UFMC modulation at millimeter wave (mmWave) frequencies have not yet been properly investigated.

This paper proposes transceiver schemes for the MIMO-UFMC modulation operating at mmWave frequencies. The contributions of this paper may be summarized as follows: (a) we provide the full mathematical model of a MIMO-UFMC scheme, taking into account the presence of hybrid analog/digital beamformers; (b) we propose several reception structures and, among these, an adaptive linear minimum mean square error (MMSE) receiver that can be implemented without resorting to an explicit channel estimation phase; (c) we propose a modified UFMC transmission scheme wherein contiguous data packets are transmitted with no guard intervals; and, finally, (d) we propose and evaluate the performance of a channel-independent pre-coding beamforming structure at the transmitter, so as to avoid the need for channel state information at the transmitter. Numerical results will show the effectiveness of the proposed transceiver algorithms and of the continuous packet transmission scheme with no guard intervals.

This paper is organized as follows. Next section contains the description of the mathematical model and of the transceiver processing for an UFMC system with multiple antennas. Section 3 contains the derivation of the linear MMSE receiver for MIMO-UFMC systems, including the definition of a channel-independent beamformer, while Sect. 4 contains the discussion of the numerical results. Finally, concluding remarks are given in Sect. 5.

2 MIMO-UFMC Transceiver Processing

In this section we generalize to the MIMO case the UFMC single-packet modulation scheme detailed in [7], presenting three different receiving structures. We will refer to the scheme reported in Fig. 1. We will denote by M the multiplexing order, by N_T and N_R the number of transmit and receive antennas, respectively, and by N_T^{RF} and N_R^{RF} the number of RF chains at the transmitter and at the receiver, respectively. We assume that the k subcarriers are split in B subbands of D subcarriers each (thus implying that $k = BD$). Assume that a sequence of Mk data symbols is to be transmitted; these symbols are arranged into an $(M \times k)$-dimensional matrix, that we denote by $\mathbf{S}$. The columns of $\mathbf{S}$ undergo a digital precoding transformation; in particular, denoting by $\mathbf{Q}_{BB}(n)$ the $(N_T^{\mathrm{RF}} \times M)$-dimensional matrix representing the digital precoder for the n-th column of $\mathbf{S}$, the useful data at the output of the digital precoding stage can be represented by the $(N_T^{\mathrm{RF}} \times k)$-dimensional matrix $\mathbf{X}$, whose n-th column, $\mathbf{X}(:, n)$ say, is expressed as $\mathbf{X}(:, n) = \mathbf{Q}_{BB}(n)\mathbf{S}(:, n)$. After digital precoding, each of the N_T^{RF} rows of the matrix $\mathbf{X}$ goes through an

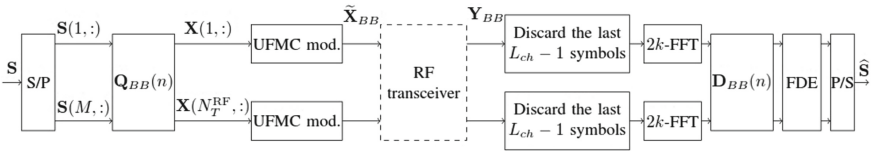

Fig. 1. Block scheme of the UFMC multi antenna transceiver. The dashed box "RF transceiver" contains the cascade of a bank of N_T^{RF} transmit shaping filters, a bank of N_T^{RF} power amplifiers, the analog RF precoding matrix $\mathbf{Q}_{\mathrm{RF}}$, the N_T transmit antennas, the $(N_R \times N_T)$-dimensional matrix-valued MIMO channel impulse response, the N_R receive antennas, the analog RF post-coding matrix $\mathbf{D}_{\mathrm{RF}}$, and a bank of N_R^{RF} receive shaping filters

UFMC modulator; the outputs of the N_T^{RF} parallel UFMC modulators can be grouped in the matrix $\widetilde{\mathbf{X}}_{BB}$ of dimension $[N_T^{\mathrm{RF}} \times (k+L-1)]$. Each UFMC modulator uses a finite impulse response (FIR) passband filter in order to improve the frequency localization property of the input signal. Denoting by $\mathbf{g} \triangleq [g_0, g_1, \ldots, g_{L-1}]^T$ the L-dimensional vector representing the prototype filter, the FIR filter used in the i-th subband to process the vector in input at the generic UFMC modulator is denoted by $\mathbf{g}_i$ and its entries $g_{i,0}, g_{i,1}, \ldots, g_{i,L-1}$ are defined as $g_{i,\ell} = g_\ell e^{j2\pi \frac{F_i \ell}{k}}$, $i = 0, \ldots, B-1$, $\ell = 0, \ldots, L-1$, with $F_i \triangleq \frac{D-1}{2} + iD$ the normalized frequency shift of the filter tuned to the i-th subband. Denoting by $\mathbf{X}(\ell,:)$ the ℓ-th row of the matrix $\mathbf{X}$, the ℓ-th row of the output matrix $\widetilde{\mathbf{X}}_{BB}$ is written as

$$\widetilde{\mathbf{X}}_{BB}(\ell,:)^T = \sum_{i=0}^{B-1} \mathbf{G}_i \mathbf{W}_{k-IFFT} \mathbf{P}_i \mathbf{X}(\ell,:)^T, \tag{1}$$

where $\mathbf{G}_i$ is the Toeplitz $[(k+L-1) \times k]$-dimensional matrix describing the discrete convolution operation with the filter $\mathbf{g}_i$, the matrix $\mathbf{W}_{k,IFFT}$ denotes the $(k \times k)$-dimensional matrix representing the isometric IFFT transformation and the $(k \times k)$-dimensional matrix $\mathbf{P}_i = \mathrm{diag}\left([\underbrace{0 \ldots 0}_{iD} \underbrace{1 \ldots 1}_{D} \underbrace{0 \ldots 0}_{k-(i+1)D}] \right)$, for $i = 0, \ldots, B-1$. Equation (1) can be compactly written in matrix notations as $\widetilde{\mathbf{X}}_{BB} = \mathbf{X} \left(\sum_{i=0}^{B-1} \mathbf{P}_i^T \mathbf{W}_{k-IFFT}^T \mathbf{G}_i^T \right)$. The columns of $\widetilde{\mathbf{X}}_{BB}$ are then fed to the MIMO RF transceiver scheme, that is made of the receive and transmit shaping filters, the analog precoding and post-coding matrices $\mathbf{Q}_{\mathrm{RF}}$ (of dimension $N_T \times N_T^{\mathrm{RF}}$) and $\mathbf{D}_{\mathrm{RF}}$ (of dimension $N_R \times N_R^{\mathrm{RF}}$), respectively, and of the MIMO channel impulse response. Assuming that the power amplifiers operate in the linear regime, the RF transceiver block can be modeled as an LTI filter with $(N_R^{\mathrm{RF}} \times N_T^{\mathrm{RF}})$-dimensional matrix-valued impulse response $\mathbf{L}(\ell) = \sqrt{P_T} \mathbf{D}_{\mathrm{RF}}^H \widetilde{\mathbf{H}}(\ell) \mathbf{Q}_{\mathrm{RF}}$, wherein P_T is the transmitted power, $\widetilde{\mathbf{H}}(\ell)$, with $\ell = 0, \ldots, L_{ch}-1$, is the matrix-valued $(N_R \times N_T)$-dimensional millimeter wave

(mmWave) channel impulse response including also the transmit and receive rectangular shaping filters [4], with L_{ch} the length of the channel impulse response (in discrete samples). The output of the RF transceiver can be represented through a matrix $\mathbf{Y}_{BB}$ of dimension $[N_R^{\mathrm{RF}} \times (k + L + L_{ch} - 2)]$. The m-th column of $\mathbf{Y}_{BB}$ is easily seen to be expressed as

$$\mathbf{Y}_{BB}(:,m)=\mathbf{D}_{\mathrm{RF}}^{H}\left[\sum_{\ell=0}^{L_{ch}-1}\sqrt{P_T}\widetilde{\mathbf{H}}(\ell)\mathbf{Q}_{\mathrm{RF}}\widetilde{\mathbf{X}}_{BB}(:,m-\ell)+\mathbf{w}(m)\right], \tag{2}$$

where we have assumed that $\widetilde{\mathbf{X}}(:,m)$ is zero for $m \leq 0$. The vector $\mathbf{w}(n)$ represents the additive thermal noise contribution. At this point, following the usual UFMC processing, the last $L_{ch} - 1$ columns of the matrix $\mathbf{Y}_{BB}$ are discarded, and each row of the resulting matrix, say $\widetilde{\mathbf{Y}}_{BB}$, is passed through an FFT on $2k$ points. The output of the FFT is downsampled by a factor of 2, so that we get a matrix of dimension $N_R^{\mathrm{RF}} \times k$, and finally, digital postcoding is applied. Denoting by $\mathbf{D}_{BB}(n)$ the $(N_R^{\mathrm{RF}} \times M)$-dimensional matrix representing the digital postcoder for the n-th column of the data matrix, we finally get a $(M \times k)$-dimensional matrix $\mathbf{Y}_{dec}$, whose n-th column can be shown to be approximately expressed as

$$\begin{aligned}\mathbf{Y}_{dec}(:,n+1) \approx \frac{2k}{\sqrt{2}}\sqrt{P_T}\mathbf{D}_{BB}^{H}(n)\mathbf{D}_{\mathrm{RF}}^{H}\overline{\mathcal{H}}(2n)\times \\ \mathbf{Q}_{RF}\mathcal{G}_{\lfloor n/D \rfloor}(2n)\mathbf{Q}_{BB}(n)\mathbf{S}(:,n+1)+\mathbf{D}_{BB}^{H}(n)\mathbf{D}_{\mathrm{RF}}^{H}\mathcal{W}(2n)\ ,\end{aligned} \tag{3}$$

with $n = 0, \ldots, k-1$. In the above equation, $\overline{\mathcal{H}}(2n)$ is an $N_R \times N_T$ matrix whose (p,q)-th entry is the $2n$-th coefficient of the isometric $2k$-point FFT of the sequence $\widetilde{\mathbf{H}}_{p,q}(0), \ldots, \widetilde{\mathbf{H}}_{p,q}(L_{ch}-1)$; similarly, $\mathcal{G}_i(2n)$ denotes the $2n$-th coefficient of the isometric $2k$-points FFT of the i-th subband filter $\mathbf{g}_i$, and $\mathcal{W}(2n)$ is an N_R-dimensional vector whose ℓ-th entry is the $2n$-th coefficient of the isometric $2k$-points FFT of the noise sequence $w_\ell(0), \ldots w_\ell\,(K + L + L_{ch} - 3)\,, \forall \ell = 1, \ldots N_{\mathrm{R}}$. We remark that (3) holds approximately and not with a perfect equality since we have discarded the last $L_{ch} - 1$ symbols. Now, given (3), an estimate of the n-th column of the data symbols matrix $\mathbf{S}$ can be simply obtained as

$$\widehat{\mathbf{S}}_{\mathrm{id}}(:,n+1) = \mathbf{E}(n+1)\mathbf{Y}_{dec}(:,n+1)\ , \tag{4}$$

where $\mathbf{E}(n+1) = \left[\frac{2k}{\sqrt{2}}\sqrt{P_T}\mathbf{D}_{BB}^{H}(n)\mathbf{D}_{\mathrm{RF}}^{H}\overline{\mathcal{H}}(2n)\mathbf{Q}_{RF}\mathcal{G}_{\lfloor \frac{n}{D} \rfloor}(2n)\mathbf{Q}_{BB}(n)\right]^{+}$, and $(\cdot)^{+}$ denotes Moore–Penrose generalized inverse.

A different processing can be obtained by avoiding the use of the approximate relation (3). We thus consider the received matrix $\mathbf{Y}_{BB}$ in Eq. (2), discard the last $L_{ch} - 1$ columns of the matrix, compute the FFT on $2k$ points, downsample the result by a factor of 2, and finally, apply digital postcoding, namely:

$$\mathbf{Y}_{\mathrm{dis}} = \mathbf{Y}_{BB}\mathbf{D}_{L_{ch}-1}\mathbf{W}_{2k,FFT}(1 : k + L - 1, :)\ , \tag{5}$$

where the matrix $\mathbf{W}_{2k,FFT}$ denotes the $(2k \times 2k)$-dimensional matrix representing the isometric FFT transformation and $\mathbf{D}_{L_{ch}-1} = [\mathbf{I}_{k+L-1}\ \mathbf{0}_{L_{ch}-1 \times k+L-1}]^{T}$

is the $[(k + L + L_{ch} - 2) \times (k + L - 1)]$-dimensional matrix used for discarding the last $L_{ch} - 1$ columns of the matrix $\mathbf{Y}_{BB}$. An estimate of the m-th column of the data symbols matrix $\mathbf{S}$ can be thus obtained as

$$\widehat{\mathbf{S}}_{\text{dis}}(:, m) = \mathbf{E}(m)\mathbf{Y}_{\text{dis}}(:, m) \; . \tag{6}$$

We can also avoid discarding the last $L_{ch} - 1$ columns of $\mathbf{Y}_{BB}$; in this case we obtain the processing

$$\widehat{\mathbf{S}}_{\text{no dis}}(:, m) = \mathbf{E}(m)\mathbf{Y}_{BB}\mathbf{W}_{2k,FFT}(1 : k + L + L_{ch} - 2, m) \; . \tag{7}$$

Equations (6) and (7), have to be computed for $m = 1, \ldots, k$.

2.1 Channel Dependent (CD) Beamformer Design

We now address the beamformers choice by referring to (3), which shows that the precoding matrices multiply by the right the FFT channel coefficient $\overline{\mathcal{H}}(2n)$, while the postcoding matrices multiply this same coefficient by the left. Denoting by $\mathbf{Q}^{\text{opt}}(n)$ and $\mathbf{D}^{\text{opt}}(n)$ the "optimal" precoding and postcoding matrices[1] for the transmission and detection of the n-th column of $\mathbf{S}$, it is seen from (3) that, upon letting $\overline{\mathcal{H}}(2n) = \overline{\mathbf{U}}(2n)\overline{\mathbf{\Lambda}}(2n)\overline{\mathbf{V}}^{H}(2n)$ be the singular-value-decomposition of $\overline{\mathcal{H}}(2n)$, the matrix $\mathbf{Q}^{\text{opt}}(n)$ should contain on its columns the M columns of $\overline{\mathbf{V}}(2n)$ associated with the largest eigenvalues of $\overline{\mathcal{H}}(2n)$, and, similarly, the matrix $\mathbf{D}^{\text{opt}}(n)$ should contain on its columns the M columns of $\overline{\mathbf{U}}(2n)$ associated with the largest eigenvalues of $\overline{\mathcal{H}}(2n)$. Given the matrices $\mathbf{Q}^{\text{opt}}(n)$ and $\mathbf{D}^{\text{opt}}(n)$, the beamformers $\mathbf{Q}_{\text{BB}}(n)$, $\mathbf{Q}_{\text{RF}}$, $\mathbf{D}_{\text{BB}}(n)$, and $\mathbf{D}_{\text{RF}}$ are obtained following the approximation algorithm reported in [6].

3 MIMO-UFMC Scheme with Linear MMSE Equalization at the Receiver

The transceiver processing described in the previous section requires the knowledge of the channel impulse response and is suited for a single packet transmission, i.e. for the case in which a single isolated block of kM symbols is transmitted. In practice, however, several blocks are to be continuously transmitted. In this case, consecutive UFMC blocks are usually spaced in discrete-time by a number of intervals equal to $L-1$ [7]; since the channel is time-dispersive, at the receiver there will be inter-block interference (IBI): in particular, the first $L_{ch}-1$ samples of the received signal $\mathbf{Y}_{BB}$ will be corrupted by the tail of the preceding block of data symbols. In this case, the single packet processing described in the previous section is suboptimal and alternative interference-suppressing schemes are to be envisaged. We now describe a linear MMSE-based processing operating directly on the matrix $\mathbf{Y}_{BB}$ reported in (2). The receiver processing is

[1] By the adjective "optimal" we mean here the beamforming matrices that we would use in the case in which the number of RF coincides with the number of antennas.

adaptive and so it, based on a known training sequence, automatically learns the interference-suppressing detection matrix; as a consequence, the detection strategy that we are going to illustrate can be used also in the case in which multiple packets are continuously transmitted, either with a guard-time between them, as recommended in [7], or with no guard-time at all. Starting from the matrix $\mathbf{Y}_{BB}$, we denote by $\mathbf{Z}_{\mathrm{BB}} = \mathbf{Y}_{BB}\mathbf{W}_{2k,FFT}(1:k+L+L_{ch}-2,:)$ the $\left(N_R^{\mathrm{RF}} \times 2K\right)$-dimensional matrix contains the $2k$-points FFT of the matrix $\mathbf{Y}_{\mathrm{BB}}$ in Eq. (2). We denote by J the number of columns of the matrix $\mathbf{Z}_{\mathrm{BB}}$ that we use to decode the symbol transmitted on the generic subcarrier, i.e., to limit system complexity, we use a window of data of dimension JN_R^{RF}. In order to estimate the symbol transmitted on the n-th subcarrier, we consider the $\left(N_R^{\mathrm{RF}} \times J\right)$-dimensional matrix $\mathbf{Z}_{\mathrm{BB}}^{(n)}$. We denote as $\mathbf{z}_{\mathrm{BB}}^{(n)}$ the vector-stacked version of $\mathbf{Z}_{\mathrm{BB}}^{(n)}$, i.e. $\mathbf{z}_{\mathrm{BB}}^{(n)} = \mathrm{vec}\left(\mathbf{Z}_{\mathrm{BB}}^{(n)}\right)$, and we consider the linear processing

$$\widehat{\mathbf{S}}_{\mathrm{mmse}}(:,n) = \mathbf{d}_{\mathrm{mmse}}(n)^H \mathbf{z}_{\mathrm{BB}}^{(n)} \,. \tag{8}$$

The detection vector can be shown to be expressed as $\mathbf{d}_{\mathrm{mmse}}(n) = \mathbf{R}_{z,n}^{-1}\mathbf{R}_{zs,n}$. In order to specify the expression of the matrices $\mathbf{R}_{z,n}$ and $\mathbf{R}_{zs,n}$, we start by considering the matrices $\widetilde{\mathbf{R}}_z$ and $\widetilde{\mathbf{R}}_{zs}$ that are obtained through time-averages approximating the matrices $\mathbf{R}_z = \mathbb{E}\left[\mathbf{z}_{\mathrm{BB}}\mathbf{z}_{\mathrm{BB}}^H\right]$ and $\mathbf{R}_{zs}^{(n)} = \mathbb{E}\left[\mathbf{z}_{\mathrm{BB}}\mathbf{S}(:,n)^H\right]$, where $\mathbf{z}_{\mathrm{BB}} = \mathrm{vec}\left(\mathbf{Z}_{\mathrm{BB}}\right)$, as follows:

$$\mathbf{R}_z \approx \widetilde{\mathbf{R}}_z = \frac{1}{N_{\mathrm{cov}}} \sum_{\ell=1}^{N_{\mathrm{cov}}} \mathbf{z}_{\mathrm{BB},\ell}\mathbf{z}_{\mathrm{BB},\ell}^H \,, \quad \mathbf{R}_{zs}^{(n)} \approx \widetilde{\mathbf{R}}_{zs}^{(n)} = \frac{1}{N_{\mathrm{cov}}} \sum_{\ell=1}^{N_{\mathrm{cov}}} \mathbf{z}_{\mathrm{BB},\ell}\mathbf{S}_\ell(:,n)^H \,. \tag{9}$$

In the above equations, N_{cov} is the number of samples used to compute the time averages, and the temporal index "ℓ" has been introduced in order to denote data coming from the ℓ-th transmitted packet. Given (9), the selection of the quantities $\mathbf{R}_{z,n}$, $\mathbf{R}_{zs,n}$ and $\mathbf{z}_{\mathrm{BB}}^{(n)}$, depends on the subcarrier index n, and the choice is made in order to select, for each n, the columns of $\mathbf{Z}_{\mathrm{BB}}$ that are most relevant for detecting the n-th column of the data matrix $\mathbf{S}$. For the sake of brevity, the full details are omitted and the main steps are summarized in Algorithm 1. The proposed procedure has a computational cost proportional to $k\left(N_R^{\mathrm{RF}}J\right)^3$, whereas the complexity of the full linear MMSE receiver, that elaborates the full matrix $\mathbf{Z}_{\mathrm{BB}}$ and corresponding to the choice $J = 2k$, the complexity climbs up to $\left[N_R^{\mathrm{RF}}\left(k+L+L_{ch}-2\right)\right]^3$.

3.1 Channel Independet (CI) Beamforming

The outlined MMSE processing relies on a sequence of pilot symbols, and does not require any prior channel estimation. Nonetheless, implementing the beamformers as outlined in Sect. 2.1 still requires knowledge of the channel state. In order to come up with a transceiver processing that does not rely on prior channel estimation, we propose a possible channel-independent beamforming scheme that can be easily implemented through the use of 0-1 switches.

Algorithm 1 Procedure for the selection of the quantities $\widetilde{\mathbf{R}}_{z,n}$, $\widetilde{\mathbf{R}}_{zs,n}$ and $\mathbf{Z}_{\mathrm{BB},n}$. The notation $\widetilde{\mathbf{R}}_z(a:b)$ denotes selection of a submatrix of $\widetilde{\mathbf{R}}_z$ containing the entries whose column and row coordinates are in the range $(a:b)$.

if $n == 1$ **or** $n == k$ **then**
  if $n == 1$ **then**
    $I_{\min,1} = 1$, $I_{\max,1} = J-2$, $I_{\min,2} = 2k-1$, $I_{\max,2} = 2k$
  else if $n == k$ **then**
    $I_{\min,1} = 1$, $I_{\max,1} = 2$, $I_{\min,2} = 2k-J+3$, $I_{\max,2} = 2k$
  end if
  $\mathbf{Z}_{\mathrm{BB}}^{(n)} = [\mathbf{Z}_{\mathrm{BB}}(:, I_{\min,1}:I_{\max,1}), \mathbf{Z}_{\mathrm{BB}}(:, I_{\min,2}:I_{\max,2})]$.
  $\mathbf{R}_{z,n} = \Big[\widetilde{\mathbf{R}}_z\left(N_R^{\mathrm{RF}}(I_{\min,1}-1)+1 : N_R^{\mathrm{RF}} I_{\max,1}\right),$
  $\widetilde{\mathbf{R}}_z\left(N_R^{\mathrm{RF}}(I_{\min,2}-1)+1 : N_R^{\mathrm{RF}} I_{\max,2}\right)\Big]$.
  $\mathbf{R}_{zs,n} = \Big[\widetilde{\mathbf{R}}_{zs}^{(n)}\left(N_R^{\mathrm{RF}}(I_{\min,1}-1)+1 : N_R^{\mathrm{RF}} I_{\max,1}, :\right),$
  $\widetilde{\mathbf{R}}_{zs}^{(n)}\left(N_R^{\mathrm{RF}}(I_{\min,2}-1)+1 : N_R^{\mathrm{RF}} I_{\max,2}, :\right)\Big]$.
else
  if $2n - \frac{J}{2} \geq 1$ **and** $2n + \frac{J}{2} - 1 \leq 2k$ **then**
    $I_{\min} = 2n - \frac{J}{2}$, $I_{\max} = 2n + \frac{J}{2} - 1$
  else if $2n - \frac{J}{2} < 1$ **then**
    $I_{\min} = 1$, $I_{\max} = J$
  else if $2n + \frac{J}{2} - 1 > 2k$ **then**
    $I_{\min} = 2k - J + 1$, $I_{\max} = 2k$
  end if
  $\mathbf{Z}_{\mathrm{BB}}^{(n)} = \mathbf{Z}_{\mathrm{BB}}\left(:, N_R^{\mathrm{RF}}(I_{\min}-1)+1 : N_R^{\mathrm{RF}} I_{\max}\right)$.
  $\mathbf{R}_{z,n} = \widetilde{\mathbf{R}}_z\left(N_R^{\mathrm{RF}}(I_{\min}-1)+1 : N_R^{\mathrm{RF}} I_{\max}\right)$.
  $\mathbf{R}_{zs,n} = \widetilde{\mathbf{R}}_{zs}^{(n)}\left(N_R^{\mathrm{RF}}(I_{\min}-1)+1 : N_R^{\mathrm{RF}} I_{\max}, :\right)$.
end if

The digital precoding $(N_T^{\mathrm{RF}} \times M)$-dimensional matrices are $\mathbf{Q}_{\mathrm{BB}}^{\mathrm{CI}}(n) = \mathbf{I}_M \otimes \mathbf{1}_{N_T^{\mathrm{RF}}/M}$ $\forall n = 1, \ldots, k$, where $\mathbf{I}_M$ is the $(M \times M)$-dimensional identity matrix and $\mathbf{1}_{N_T^{\mathrm{RF}}/M}$ is the $\frac{N_T^{\mathrm{RF}}}{M}$-dimensional vector whose entries are all equal to 1, and $\otimes$ denotes the Kronecker product. Notice also that the above defined digital precoding matrices are no longer dependent on the subcarrier index. The analog precoding $(N_T \times N_T^{\mathrm{RF}})$- dimensional matrix is $\mathbf{Q}_{\mathrm{RF}}^{\mathrm{CI}} = \mathbf{I}_{N_T^{\mathrm{RF}}} \otimes \mathbf{1}_{N_T/N_T^{\mathrm{RF}}}$, and the analog postcoding $(N_R \times N_R^{\mathrm{RF}})$- dimensional matrix is $\mathbf{D}_{\mathrm{RF}}^{\mathrm{CI}} = \mathbf{I}_{N_R^{\mathrm{RF}}} \otimes \mathbf{1}_{N_R/N_R^{\mathrm{RF}}}$.

4 Performance Measures and Numerical Results

In order to evaluate the performance of the transceiver architectures proposed in the paper, we will three different figures of merit. The first one is the root mean square error (RMSE) defined as $\mathrm{RMSE} = \mathbb{E}\left[\frac{|s-\hat{s}|^2}{|s|^2}\right]$, where s and $\hat{s}$ are the generic symbol transmitted and estimated, respectively.

The second one is the bit-error-rate (BER), while, finally, the third one is the throughput, that is measured in bit/s, and depends on the system BER

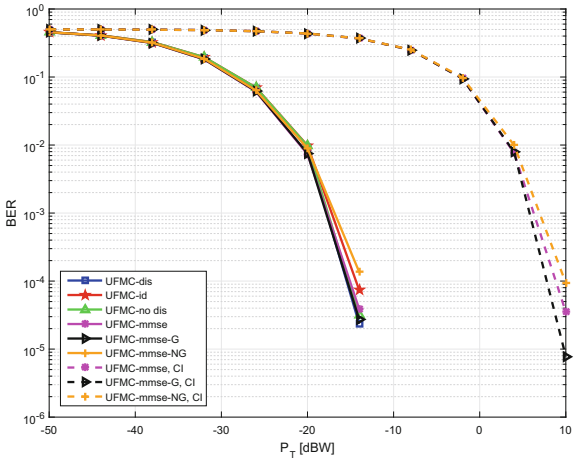

Fig. 2. BER versus transmit power with $M = 1$, performance of MIMO-UFMC transceiver architectures with CD and CI beamformers

and on the cardinality of the used modulation. Denoting by T_s the signaling time, i.e. assuming that the modulator transmits a data-symbol of cardinality $\mathcal{M}$ every T_s seconds, kM symbols are transmitted in $(k + L - 1)T_s$ seconds, in the case in which we consider the guard intervals in the packet transmission, and in kT_s seconds, in the case in which we do not consider the guard intervals between the consecutive blocks. Denoting by W the communication bandwidth, the throughputs $\mathcal{T}_{\mathrm{G}}$ and $\mathcal{T}_{\mathrm{NG}}$ are expressed as

$$\mathcal{T}_{\mathrm{G}} = \frac{W \log_2(\mathcal{M})\, kM}{k + L - 1}(1 - \mathrm{BER})\,, \qquad \mathcal{T}_{\mathrm{NG}} = W \log_2(\mathcal{M})\, M(1 - \mathrm{BER}) \quad [\mathrm{bit/s}]\,. \tag{10}$$

when we consider the guard interval between packets or not, respectively.

In our simulation setup, we consider a communication bandwidth of $W = 500\,\mathrm{MHz}$ centered over a mmWave carrier frequency. The MIMO propagation channel has been generated according to the statistical procedure described in [3,4]. We assume a distance between transmitter and receiver of 50 m. The additive thermal noise is assumed to have a power spectral density of $-174\,\mathrm{dBm/Hz}$, while the front-end receiver is assumed to have a noise figure of 3 dB. For the prototype filter in the UFMC modulators we use a Dolph–Chebyshev filter with length $L = 16$ and side-lobe attenuation with respect to the peak of the main lobe equal to 100 dB. We use $k = 128$ subcarriers, $B = 8$ subbands (which leads to $D = 16$ subcarriers in each subband), and we assume 4-QAM modulation. We consider the antenna configuration $N_R \times N_T = 16 \times 64$, and we assume hybrid beamforming with $N_T^{\mathrm{RF}} = 16$ and $N_R^{\mathrm{RF}} = 4$. In the figures we denote as "UFMC-id" the case in which the estimate of the n-th column of the data symbols matrix $\mathbf{S}$ is expressed as (4), as "UFMC-dis" the case in which we use (6), as "UFMC-no dis" the case in which we use (7), as "UFMC-mmse" the case in which we use (8). With regard to the continuous packet transmis-

sion, we label with "UFMC-mmse-G" the case in which we use $L-1$ guard intervals between consecutive packets and with "UFMC-mmse-NG" the case without guard intervals between them.

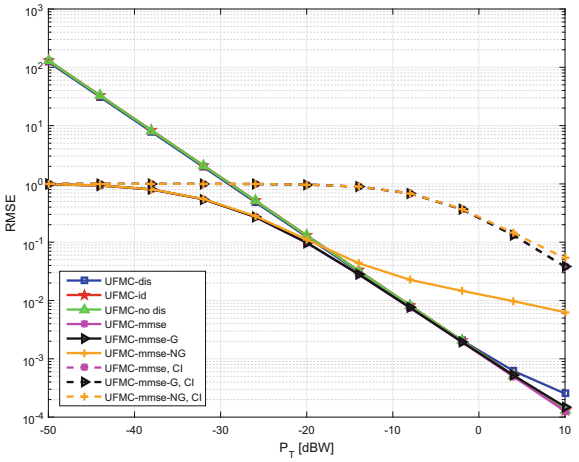

Fig. 3. RMSE versus transmit power with $M = 1$, performance of MIMO-UFMC transceiver architectures with CD and CI beamformers.

In Figs. 2, 3, and 4 we show the BER, the RMSE and the throughput versus the transmit power, for the case $M = 1$, considering the hybrid implementation of CD and CI beamformers. The obtained results show that the performances of the "UFMC-mmse" are superior to the ones offered by the standard MIMO-UFMC, even using beamformers based on the ideal received channel model in Eq. (3) and described in Sect. 2.1. This behaviour can be justified by the fact that the MMSE-based receiver described here performs an online MMSE detection of the data symbols, automatically rejecting the interference contribution. We can see that in terms of BER and RMSE the performances of "UFMC-mmse-NG" are worse than the ones obtained with "UFMC-mmse-G", because of the increased overlap (i.e., interference) of the data corresponding to consecutive blocks. Nevertheless, the throughput of "UFMC-mmse-NG" is larger than that obtained with the "UFMC-mmse-G", i.e., the increase in the system BER due to increased interference is compensated by the increased efficiency due to the fact that there are no guard intervals. For the case in which transmitter and receiver have no CSI, the CI beamformers of Sect. 3.1 are employed.

5 Conclusions

This paper presented several signal processing schemes have been developed for data detection in MIMO-UFMC systems, taking into account also the hybrid nature of the beamformers. In particular, an adaptive MMSE receiver has been

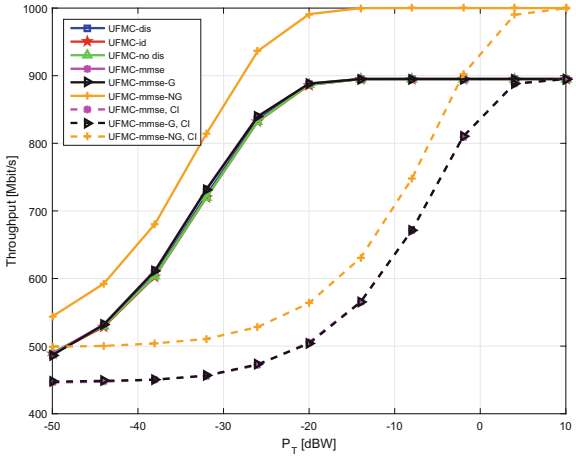

Fig. 4. Throughput versus transmit power with $M = 1$, performance of MIMO-UFMC transceiver architectures with CD and CI beamformers.

proposed that, in conjunction with CI beamforming, does not require prior channel estimation. This receiver, for the case in which no guard-time is inserted between consecutive packets at the transmitter, has been shown to be able to achieve increased performance in terms of system throughput.

References

1. Abdoli, J., Jia, M., Ma, J.: Filtered OFDM: a new waveform for future wireless systems. In: 2015 IEEE 16th International Workshop on Signal Processing Advances in Wireless Communications (SPAWC), pp. 66–70 (2015). https://doi.org/10.1109/SPAWC.2015.7227001
2. Banelli, P., Buzzi, S., Colavolpe, G., Modenini, A., Rusek, F., Ugolini, A.: Modulation formats and waveforms for 5G networks: who will be the heir of OFDM? IEEE Signal Process. Mag. **31**(6), 80–93 (2014)
3. Buzzi, S., D'Andrea, C.: On clustered statistical MIMO millimeter wave channel simulation (2016). https://arxiv.org/abs/1604.00648
4. Buzzi, S., D'Andrea, C., Foggi, T., Ugolini, A., Colavolpe, G.: Single-carrier modulation versus OFDM for millimeter-wave wireless MIMO. IEEE Trans. Commun. **66**, 1335–1348 (2018). https://doi.org/10.1109/TCOMM.2017.2771334
5. Farhang-Boroujeny, B.: OFDM versus filter bank multicarrier. IEEE Signal Process. Mag. **28**(3), 92–112 (2011)
6. Ghauch, H., Kim, T., Bengtsson, M., Skoglund, M.: Subspace estimation and decomposition for large millimeter-wave MIMO systems. IEEE J. Sel. Top. Signal Process. **10**(3), 528–542 (2016). https://doi.org/10.1109/JSTSP.2016.2538178
7. Vakilian, V., Wild, T., Schaich, F., ten Brink, S., Frigon, J.F.: Universal-filtered multi-carrier technique for wireless systems beyond LTE. In: 2013 IEEE Globecom Workshops (GC Wkshps), pp. 223–228 (2013). https://doi.org/10.1109/GLOCOMW.2013.6824990